

# Path Variation and Image Segmentation

Pablo Andrés Arbeláez and Laurent D. Cohen

CEREMADE, UMR CNRS 7534 Université Paris Dauphine,  
Place du maréchal de Lattre de Tassigny,  
75775 Paris cedex 16, France  
arbelaez@ceremade.dauphine.fr, cohen@ceremade.dauphine.fr

**Abstract.** We study a notion of variation for real valued two variable functions called the *path variation* and we discuss its application as a low-level image segmentation method. For this purpose, we characterize the path variation as an energy in the framework of minimal paths. In this context, the definition of an energy and the selection of a set of source points determine a partition of the image domain. The problem of choosing a relevant set of sources is addressed through a nonlinear diffusion filtering.

## 1 Introduction

The notion of *variation* or *total variation* for functions of one real variable was introduced by C. Jordan [12] as early as in 1881. This functional has found application in various branches of mathematics [17, 18], particularly, in the definition of the Stieltjes integral. In the regular framework, the variation of a function  $f : [0, L] \rightarrow \mathbb{R}$  can be written as [11]:

$$v(f) = \int_0^L |f'(s)| ds . \quad (1)$$

Several definitions of the variation have been proposed for functions of multiple variables; if  $u : \Omega \subset \mathbb{R}^2 \rightarrow \mathbb{R}$  is a smooth function, a natural generalization of (1) consists in replacing the derivative by the gradient:

$$V(u) = \int_{\Omega} \|\nabla u(x)\| dx . \quad (2)$$

In the context of image analysis, the general version of (2), allowing discontinuities in the function, was first considered by Osher and Rudin [19, 21]. In the last decade, the representation of an image as the sum of one term of bounded variation and one term due to noise has been widely adopted. Methods based on the minimization of the total variation have been successfully applied for image restoration and denoising purposes [22, 5, 3, 9].

In this paper, we study a notion of variation for real valued functions of two variables that, in contrast to the usual total variation, is defined pointwise. Precisely, we define the *path variation* between two points of the domain as

the minimal total variation of the function on all the paths that join them. Furthermore, we propose a discrete interpretation of the path variation and we discuss its application as a low-level segmentation tool.

Image segmentation is a fundamental issue in the field of computer vision. Its great complexity may be understood by the fact that partitioning an image domain into "meaningful" regions requires a level of interpretation of the image information. Therefore, the introduction of prior knowledge seems unavoidable in the segmentation process. However, a first pre-cognitive task is the extraction of the image structure provided by low-level cues.

In order to apply the path variation to the segmentation of monochrome images, we characterize this notion as an energy in the framework of minimal paths. In this context, an energy determines a partition of the image domain by considering the influence zones of a set of source points.

Then, we address the problem of selecting a set of sources that represent accurately the image structure. For this purpose, we consider the intensity extrema of a scale-space representation of the image.

This paper is organized as follows: the basic definitions of the minimal paths approach are given in Sect. 2. The path variation is presented in Sect. 3. In Sect. 4, we discuss the choice of a set of source points.

## 2 Definitions

This introductory section presents the general framework for the rest of the paper. Basic definitions are recalled and the notations settled.

### 2.1 Minimal Paths

Let  $\Omega \subset \mathbb{R}^2$  be a compact connected domain in the plane and  $x, y \in \Omega$  two points. A *path* from  $x$  to  $y$  designates an injective  $\mathcal{C}^1$  function  $\gamma : [0, L] \rightarrow \Omega$  such that  $\gamma(0) = x$  and  $\gamma(L) = y$ . The image of  $\gamma$  is then a rectifiable simple curve in the domain. The path is parameterized by the arclength parameter  $s$ , i.e:  $\|\dot{\gamma}(s)\| = 1, \forall s \in [0, L]$  and  $L$  represents the Euclidean length of the path. The set of paths from  $x$  to  $y$  is noted by  $\Gamma_{xy}$ .

**Definition 1.** *The **surface of minimal action, or energy**, of a potential function  $P : \Omega \times \mathcal{S}^1 \rightarrow \mathbb{R}^+$ , with respect to a source point  $x_0 \in \Omega$ , evaluated at  $x$ , is defined as*

$$E_0(x) = \inf_{\gamma \in \Gamma_{x_0 x}} \int_0^L P(\gamma(s), \dot{\gamma}(s)) ds .$$

When  $P$  depends only on the position  $\gamma(\cdot)$  and is strictly positive, the field of geometrical optics provides the following physical interpretation of the energy: the potential  $P : \Omega \rightarrow \mathbb{R}^+$  represents a refractive field of indices of an optical medium and  $E_0$ , called the *eikonal* in this context, supplies the optical length

of the light rays. Then, the relation between the energy and the potential can be expressed by the *Eikonal Equation*:

$$\|\nabla E_0(x)\| = P(x) \ , \quad (3)$$

with boundary condition  $E_0(x_0) = 0$ .

In this particular case, the computation of the energy can be performed using Sethian's *Fast Marching* method [23, 7]. Noticing that the information is propagating outwards from the sources, the Fast Marching uses an up-wind scheme to construct a correct approximation of the viscosity solution of (3).

Energy minimizing paths have been used to address several problems in the field of computer vision, where the potential is generally defined as a function of the image. Examples include the global minimum for active contour models [7], shape from shading [13], continuous scale morphology [14], virtual endoscopy [8] and perceptual grouping [6].

## 2.2 Energy Partitions

The energy with respect to a set of sources  $S = \{x_i\}_{i \in J}$  is defined as the minimal individual energy:

$$E_S(x) = \inf_{i \in J} E_i(x) \ .$$

In the presence of multiple sources, a valuable information is provided by the interaction in the domain of a source  $x_i$  with the other elements of  $S$ , which is expressed through its *influence zone*:

$$Z_i = \{x \in \Omega \mid E_i(x) < E_j(x), \forall j \in J, j \neq i\} \ .$$

Thus, the influence zone, or briefly the *zone*, is a connected subset of the domain, completely determined by the energy and the rest of the sources. Their union is noted by:

$$Z(E, S) = \bigcup_{i \in J} Z_i \ .$$

The *medial set* is defined as the complementary set of  $Z(E, S)$ :

$$M(E, S) = \{x \in \Omega \mid \exists i, j \in J, i \neq j : E_S(x) = E_i(x) = E_j(x)\} \ .$$

**Definition 2.** *The energy partition of a domain  $\Omega$  with respect to an energy  $E$  and a set of sources  $S$ , is defined as:*

$$\Pi(E, S) = Z(E, S) \bigcup M(E, S) \ .$$

As a first example, if the potential is constant, e.g.  $P \equiv 1$ , then the energy at  $x$ ,

$$G_0(x) = \inf_{\gamma \in \Gamma_{x_0 x}} \int_0^L ds \ ,$$

becomes the geodesic distance to the source, or the Euclidean length of the shortest path between  $x_0$  and  $x$ . Moreover, if the domain is convex, then  $G_0$  coincides with the usual Euclidean distance to  $x_0$ . If a set of sources  $S = \{x_i\}_{i \in J}$  is considered, then the medial set  $M(G, S)$  corresponds to the Voronoi diagram and the zones  $Z(G, S)$  to the Voronoi cells.

### 2.3 Mosaic Images

Therefore, in this context, the image segmentation problem is transferred to the definition of an energy from the image data and the selection of a set of sources. Nevertheless, in practice, digital images are subsampled on the discrete grid. Consequently, important parts of the medial set often fall in the intergrid space. For region based segmentation purposes, an alternative to surround this problem is to consider an energy partition composed only by zones. Thus, the elements of the medial set that would fall exactly in the grid are assigned to one of their neighboring influence zones.

Then, an approximation of the image can be constructed by the assignation of a *model* to represent each influence zone. The model is determined by the distribution of the image values on the zone; simple models are the mean or median value on the influence zone and source's level. When the model is constant, the valuation of each zone by its model produces a piecewise constant approximation of the image, referred in the sequel as a *mosaic image*.

## 3 The Path Variation

In the usual approach for the application of minimal paths to image analysis, a large part of the problem consists in the design of a relevant potential for a specific situation and type of images. However, we adopt a different perspective and use the framework of the previous section for the study of a particular energy, whose definition depends only on geometric properties of the image.

### 3.1 Continuous Domain

Jordan introduced the notion of variation for functions of one real variable as follows [12]:

Let  $f : [0, L] \rightarrow \mathbb{R}$  be a function,  $\sigma = \{s_0, \dots, s_n\}$  a finite partition of  $[0, L]$  such that  $0 = s_0 < s_1 < \dots < s_n = L$  and  $\Phi$  the set of such partitions.

The *total variation* of  $f$  is defined as the (possible infinite) number given by the formula:

$$v(f) = \sup_{\sigma \in \Phi} \sum_{i=1}^n |f(s_i) - f(s_{i-1})| .$$

Hence, for two variable functions, we consider the minimal total variation on all the paths that join two points of the domain [1]:

**Definition 3.** The *path variation* of a function  $u : \Omega \subset \mathbb{R}^2 \rightarrow \mathbb{R}$  with respect to a source point  $x_0 \in \Omega$ , evaluated at  $x$ , is defined as

$$V_0(u)(x) = \inf_{\gamma \in \Gamma_{x_0 x}} v(u \circ \gamma) .$$

**Definition 4.** The space of functions of *bounded path variation* of  $\Omega$ , noted by  $BPV(\Omega)$  is defined by

$$BPV(\Omega) = \{u : \Omega \rightarrow \mathbb{R} \mid \forall x_0, x \in \Omega, \exists \hat{\gamma} \in \Gamma_{x_0 x} : V_0(u)(x) = v(u \circ \hat{\gamma}) < \infty\} .$$

In the sequel, we suppose that  $u$  has bounded path variation. Note that, if  $u \in BPV(\Omega)$ , then the path variation of  $u$  between any couple of points is not only required to be finite but also to be realized by a path. Hence, Def. 4 supposes the existence of geodesics for  $V$ . This assumption seems reasonable for digital images; however, it should be noted that the geodesics of the path variation are generally not unique:

A path  $\gamma \in \Gamma_{xy}$  is said to be *monotone* for  $u$  if  $u \circ \gamma$  is a monotone function. By definition, if a path is monotone for  $u$ , then it is a geodesic for  $V(u)$ . Conversely, every geodesic for  $V(u)$  is a concatenation of monotone paths.

In the regular framework, the path variation can be characterized as an energy, in the sense of Def. 1 :

**Proposition 1.** If  $u \in \mathcal{C}^1(\Omega) \cap BPV(\Omega)$ , then the path variation  $V_0(u)$  is the surface of minimal action of the potential  $P = |D_\gamma u|$ , the absolute value of the directional derivative of  $u$  in the tangent direction of the path.

*Proof.* If  $f \in \mathcal{C}^1([0, L])$ , then the total variation can be expressed in terms of its derivative [11] by the formula:

$$v(f) = \int_0^L |f'(s)| ds .$$

Thus, if  $u$  is a continuously differentiable function, Def 3. can be reformulated as:

$$V_0(u)(x) = \inf_{\gamma \in \Gamma_{x_0 x}} \int_0^L \left| \frac{\partial(u \circ \gamma)}{\partial s}(s) \right| ds .$$

Hence, we obtain the following expression for the path variation:

$$V_0(u)(x) = \inf_{\gamma \in \Gamma_{x_0 x}} \int_0^L |D_\gamma u(\gamma(s))| ds .$$

□

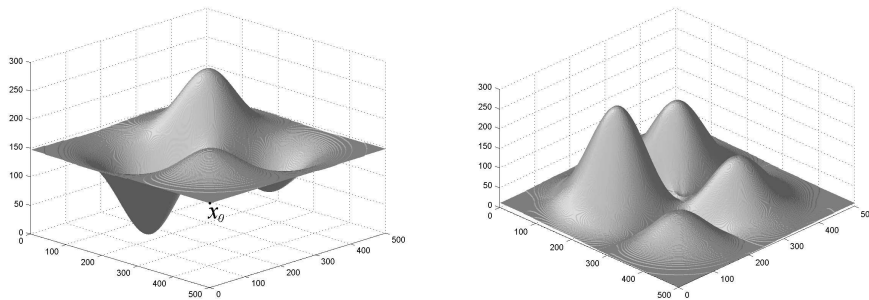


**Fig. 1.** Simple example: graphs of  $u$  and  $V_0(u)$ .

The intuitive interpretation of the path variation is illustrated in Fig. 1: consider a particle moving along the graph of the function depicted on the left and starting at the source  $x_0$ . Then, as shown on the right, the value of  $V_0(u)$ , evaluated at  $x$ , represents the minimal sum of ascents and descents to be travelled to reach the point  $x$ .

The path variation expresses the same geometric notion as the *linear variation*, introduced in [15], though in a different formulation, as a part of a geometric theory for functions of two variables.

The *component* of  $u$  containing  $x$ , noted by  $K_x$ , designates the maximal connected subset of  $\Omega$  such that  $u(y) = u(x)$ ,  $\forall y \in K_x$ . The level of a component  $K$  is noted by  $u(K)$  and the set of components of  $u$  is noted by  $T_u$ . The components of a continuous function are closed and pairwise disjoint subsets of  $\Omega$ . For continuously differentiable functions, the components of the nonsingular levels (i.e.: levels  $t$  such that  $0 \notin \nabla u(u^{-1}(t))$ ) coincide with the level lines of  $u$  and can be described as Jordan curves.

The importance of the components for the path variation is expressed by the following proposition, whose proof is an immediate consequence of Def. 3.

**Proposition 2.** *The path variation acts on the component space  $T_u$ :*

$$\forall x, y \in \Omega, K_x = K_y \Rightarrow \forall x_0, V_0(u)(x) = V_0(u)(y) .$$

Therefore, each component of  $V_0(u)$  is a union of components of  $u$ . Furthermore, for a set of sources  $S$ , each element of  $\Pi(V(u), S)$  is a union of components of the function. Thus, since the energy partitions induced by the path variation preserve this geometric structure of the function,  $V(u)$  presents a particular interest for image analysis. Additionally, the energy partitions induced by the path variation are invariant under linear contrast changes.

Figure 2 illustrates the application of the path variation on two different test functions. On the top row, a smooth function, given by the simple formula

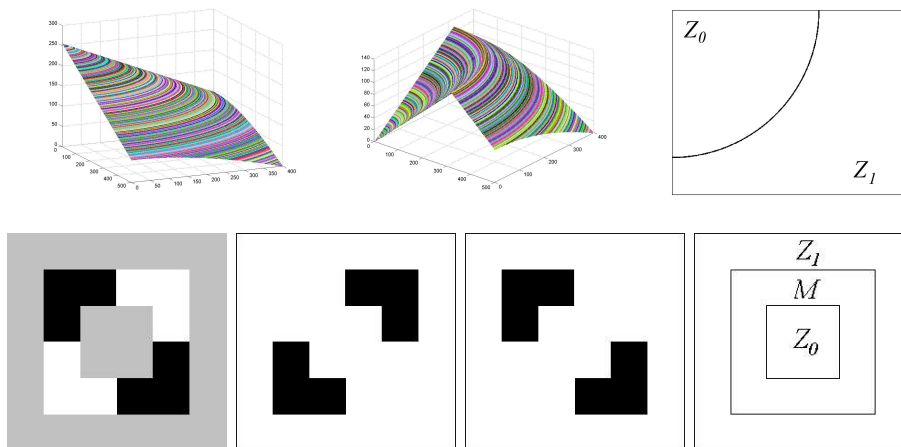


**Fig. 2.** Energy partitions of the path variation for two different test functions (see text).

$u(x) = c\|x - x_0\|$ . The set of sources  $S = \{x_0, x_1\}$ , is composed by the upper left and the lower right corners of the domain. From left to right, we can observe the graph of  $u$ , the graph of  $V_S(u)$  and the energy partition  $\Pi(V(u), S)$ . In this case, the components of the function are nested and the medial set  $M(V(u), S)$ , shown in black, corresponds to the component whose level is the average of the sources' levels.

In contrast, the function on the bottom-left of Fig. 2 is piecewise constant; the corresponding gray levels were set to 0 for the black, 254 for the white and 127 for the gray. The two images on the middle show, in black, the level sets  $[u \geq 200]$  and  $[u \leq 100]$  respectively. Finally, bottom-right displays the energy partition obtained by taking the two gray components as sources. Notice that the component spaces of the two functions have different topologies. As a consequence, in the second example, even if the boundaries of the zones are composed by pieces of level lines, none of the squares determined by the energy partition is a level line of the function.

### 3.2 Discrete Domain

In this paragraph, we propose a discrete interpretation for the path variation. Thus, we consider that the image  $u$  has been sampled on a uniform grid. A first remark is that, since the potential of the path variation in Prop. 1 depends not only on the position but also on the path direction, the Fast Marching method cannot be used for its implementation.

Nevertheless, in a discrete domain, the component structure of a function can be represented by an adjacency graph  $G$ , where the nodes correspond to discrete components and the links join neighboring components. Thus,  $G$  is the

equivalent of  $T_u$  in the discrete space. Since  $V$  acts on the components of the function, we propose to construct the discrete path variation directly on  $G$ .

A path on  $G$  joining the components of two points  $p$  and  $q$  is a set  $\gamma = \{K_0, \dots, K_n\}$  such that  $K_p = K_0$ ,  $K_n = K_q$ ,  $K_i$  and  $K_{i-1}$  are neighbors,  $\forall i = 1, \dots, n$ . The set of such paths is noted by  $\Gamma_{pq}^G$ . Each element of  $\Gamma_{pq}^G$  corresponds then to a class of discrete paths between  $p$  and  $q$ .

Thus, the expression of the discrete path variation of  $u$  at a point  $q$  with respect to the source  $p$  becomes

$$V_p(u)(q) = \min_{\gamma \in \Gamma_{pq}^G} \sum_{i=1}^n |u(K_i) - u(K_{i-1})| .$$

Hence, the calculation of  $V_p(u)$  is reduced to finding the path of minimal cost on a graph. This classical problem can be solved using a greedy algorithm [10, 16]. The complexity of this straightforward implementation for the path variation is then  $O(N \log(N))$ , where  $N$  is the total number of discrete components of the image. Furthermore, if  $u$  takes integer values, the sorting step in the update of the narrow band can be suppressed and the complexity is reduced to  $O(N)$ .

## 4 Sources Selection

In order to use a surface of minimal action to address image segmentation problems, the choice of the sources is a critical issue. Indeed, since Def. 1 is based on an integration along the paths, the partitions determined by this type of energies are very sensitive to the location of the sources. Furthermore, replacing a source  $x_i \in S$  by another point  $x'_i \in Z_i$  usually modifies the corresponding energy partition.

Therefore, the set of sources must be physically representative of the image content. Ideally, for region based segmentation purposes, each zone should correspond to a meaningful feature in the image and their boundaries should coincide with the contours of the objects.

A first option is to address the problem interactively. In this case, a human operator decides which are the meaningful features in the image and the path variation is used to determine their contours. Thus, with this approach, the choice of the sources can be seen as the moment where semantic information is introduced in the segmentation process. This idea was also used in the well known *markers* method related to the watershed transform [2].

Figure 3 displays, on the left, a set  $S$ , composed by 25 hand-placed sources for the *cameraman* test image. The source points, represented by white disks for better visualization, were chosen to provide a general description of the image, while including perceptually important details such as the face, the camera or the building on the background. On the right, we can observe the energy partition  $\Pi(V(u), S)$ . Note how the boundaries of the zones model accurately the contour information and, particularly, semantically important characteristics of edges such as corners and junctions.

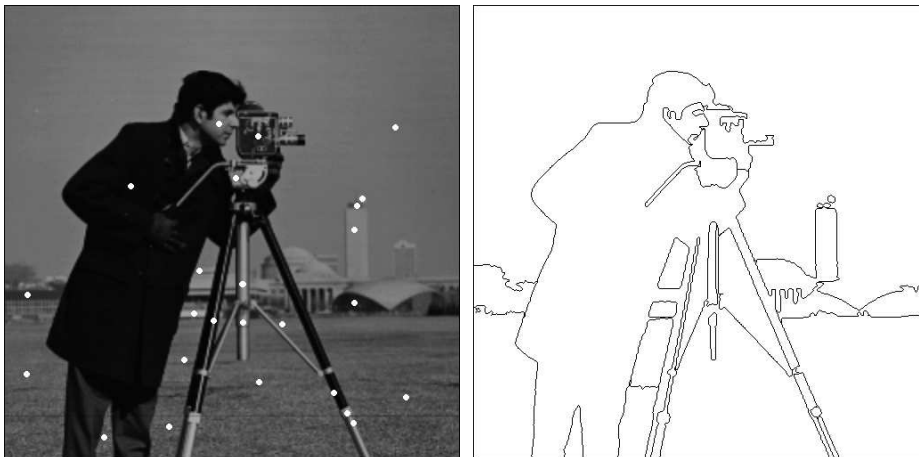


**Fig. 3.** Example of hand-placed sources and corresponding energy partition.

#### 4.1 The Extrema Partition

A different problem is the choice of a set of sources without the intervention of a human operator. Figure 4 exemplifies this issue on the smooth image  $u$  on top-left. An acceptable segmentation of this "scene" should be composed by four approximately circular regions on a gray background. A solution is to consider the extrema of the four peaks as sources for the "features" and the border of the domain as the source representing the background. The image on top-right shows the set of sources,  $S$ , and the corresponding energy partition. On bottom-left, we can observe the graph of the energy  $V_S(u)$ . Finally, on bottom-right, we observe the corresponding mosaic image, when the zone model is intensity at the source.

Therefore, in the regular framework, the image extrema appear as natural candidates for the sources. The energy partition induced by the path variation and the set of extremal components,  $\Pi(V(u), ext(u))$ , will be called the *extrema partition* of the image  $u$  and the corresponding mosaic image, the *extrema mosaic*.

In real images, the choice of the path variation as the energy and the spatial distribution of the intensity extrema provide a compromise between content conservation and simplification in the extrema mosaic. This piecewise constant approximation of the image can be seen as a decomposition in elemental zones or as a first abstraction of the image information. The extrema mosaic may be used as a parameter-free presegmentation, where the contour information is preserved.

In certain cases, it may prove useful to repeat the process and construct the extrema mosaic of an extrema mosaic. However, an excessive iteration destroys the physical meaning of the intensity extrema and often results in an alteration of the original image structure.

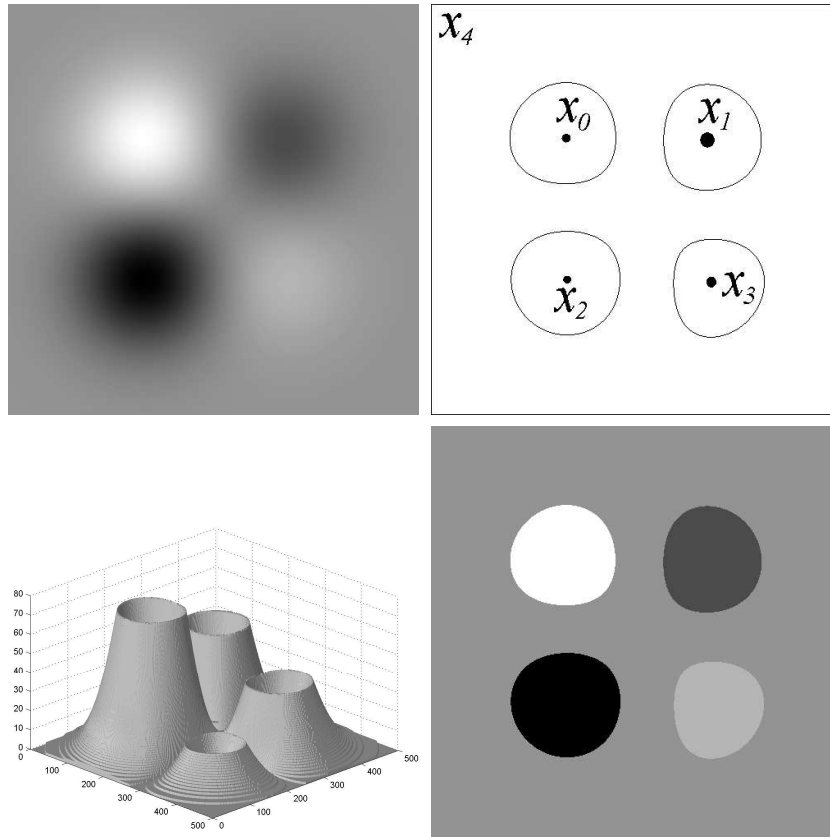


**Fig. 4.** Top: original image and energy partition. Bottom: graph of the energy and mosaic image.

Figure 5 shows an example where the extrema mosaic was applied two times on a natural image. The ratio between the number of components in the original image and the final number of zones is in this case 42.35. On the left, we can observe the original image and, on the right, the second extrema mosaic. This image illustrates two properties of the extrema partition. First, an enhancement of the contrast information, as can be seen on the butterfly's wings. Second, a reduction of the blur in the background, caused by the absorption of blurred contours and transition components by neighboring zones.

## 4.2 Nonlinear Diffusion Filtering

Frequently, the presence of textures and noise in natural images produces a large number of extrema in the intensity. Consequently, the extrema partition is often composed by a great quantity of small zones. The question is then how to reduce the number of extrema while preserving the image structure. In [25],



**Fig. 5.** Original image and extrema mosaic.

the authors proposed to preprocess the image with methods based on partial differential equations, in order to improve the watershed segmentation. In this paragraph, we discuss the use of a scale-space representation of the image to select the sources for our approach.

Thus, we consider the regularized version [4, 24] of the classical approach proposed by Perona and Malik [20]. In this method, a filtered image  $u_t = u(x, t)$  is constructed as a solution of the nonlinear diffusion equation:

$$\frac{\partial u}{\partial t} = \text{div}(g(|\nabla(G_\sigma * u)|^2)\nabla u) , \quad (4)$$

where  $G_\sigma$  denotes a Gaussian kernel of variance  $\sigma$  and  $g(\cdot)$  is a positive *diffusivity function*. Reflecting boundary conditions are considered and the initial state  $u_0 = u(x, 0)$  coincides with the original image.

For the examples presented, we used the diffusivity :

$$g(s) = \begin{cases} 1, & \text{if } s \leq 0 \\ 1 - \exp\left(\frac{-3.315}{(s/\kappa)^4}\right), & \text{if } s > 0 \end{cases}$$

where  $\kappa$  is the contrast parameter that regulates the selective smoothing process. This diffusivity was reported in [26] to lead to better results than the original functions in [20].

The main properties of nonlinear diffusion filtering are illustrated in Fig. 6. The initial image  $u_0$  was the extrema mosaic of the *cameraman*, shown on the left. The parameters of the diffusion were  $\sigma = 1$  and  $\kappa = 30$ . The filtered image  $u_t$ , shown on the right, corresponds to the scale  $t = 180$ . In this method, intraregional smoothing is preferred to interregional smoothing. Thus, homogeneous regions are smoothed in the filtered image  $u_t$ , while the edge information is enhanced.

Therefore, the number of extrema in the filtered image, noted by  $\text{ext}(u_t)$ , decreases rapidly when the scale is augmented. These properties make of  $\text{ext}(u_t)$



**Fig. 6.** Example of nonlinear diffusion filtering (see text).

an interesting candidate for the set of sources of our energy partitions. Two choices are then possible, either consider the extrema partition of the filtered image,  $\Pi(V(u_t), ext(u_t))$ , or go back to the initial image  $u_0$  and construct the partition  $\Pi(V(u_0), ext(u_t))$ .

Figure 7 illustrates this method for the choice of the sources, with the example of Fig. 6. The number of extremal components decreased from 8412 in the original image to 261 in the smoothed image. Top-left shows the extrema mosaic of  $u_t$  and top-right displays the mosaic image of  $\Pi(V(u_0), ext(u_t))$ . Notice how both energy partitions, shown on the bottom row, preserve the image structure, in spite of the reduction in the number of sources. The main difference lies in the regularization of the zones in the filtered image with respect to the zones obtained with the initial image.

In summary, the use of nonlinear diffusion produces in general a representative set the sources. However, an excessive filtering destroys the contour information. Thus, this method requires the tuning of the diffusion parameters. Finally, note that even homogeneous regions like the sky in Fig. 7 contain several extrema after the filtering.

The comparison between the results of Fig. 7 and the partition obtained with hand-placed sources in Fig. 3 suggests that other approaches for the choice of the sources may lead to better results.

Alternatively, our approach can be seen as a parameter-free method to construct a partition with a small number of regions, starting from an image filtered by nonlinear diffusion.

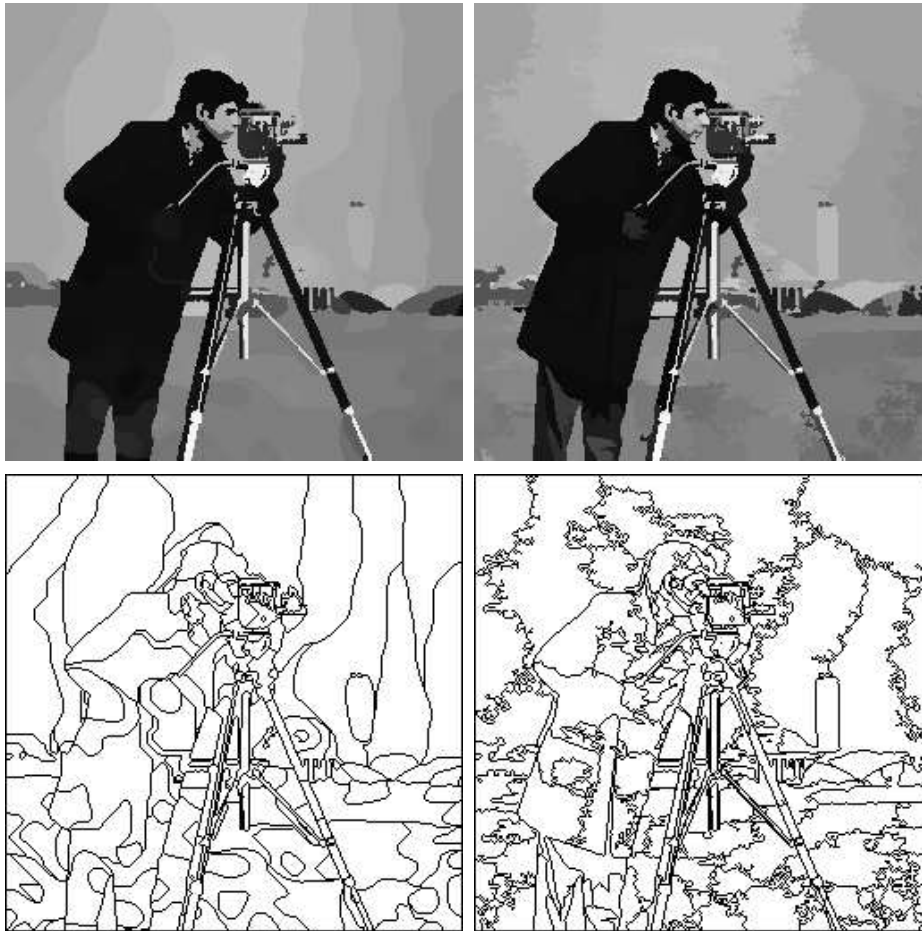


Fig. 7. Sources selection by nonlinear diffusion (see text).

## 5 Conclusion and Perspectives

In this paper, we discussed the application of the path variation to the segmentation of monochrome images. It should be noted that the use of the path variation for the construction of an energy partition assumes a certain homogeneity of the objects represented in the image. Therefore, in order to apply this approach to highly textured or noisy images, a pre-processing step should be considered.

Finally, present work includes the generalization of our approach to vector-valued images and the definition of alternative methods for the selection of the sources.

## Acknowledgments

The first author wishes to thank P. Monasse and J.M. Morel for introducing him to the inspiring work of A.S. Kronrod.

## References

1. P. A. Arbeláez. The path variation. Technical report, CEREMADE, 2003.
2. S. Beucher and F. Meyer. The morphological approach to segmentation: The watershed transformation. *Mathematical Morphology in Image Processing*, pages 433–481, 1992.
3. P. Blomgren and T.F. Chan. Color tv: Total variation methods for restoration of vector-valued images. *IP*, 7(3):304–309, March 1998.
4. F. Catté, P. L. Lions, J. M. Morel, and T. Coll. Image selective smoothing and edge detection by nonlinear diffusion. *SIAM J. Numer. Anal.*, 29(1):182–193, 1992.
5. A. Chambolle and P.L. Lions. Image recovery via total variation minimization and related problems. *Numerische Mathematik*, 76:167–188, 1997.
6. L. D. Cohen. Multiple contour finding and perceptual grouping using minimal paths. *Journal of Mathematical Imaging and Vision*, 14(3):225–236, 2001.
7. L. D. Cohen and R. Kimmel. Global minimum for active contour models: A minimal path approach. *International Journal of Computer Vision*, 24(1):57–78, August 1997.
8. T. Deschamps and L. D. Cohen. Fast extraction of minimal paths in 3d images and applications to virtual endoscopy. *Medical Image Analysis*, 5(4):281–299, 2001.
9. F. Dibos and G. Koepfler. Global total variation minimization. *SIAM Journal of Numerical Analysis*, 37(2):646–664, 2000.
10. E. W. Dijkstra. A note on two problems in connection with graphs. *Numerische Mathematik*, 1:269–271, 1959.
11. E. Hewitt and K. Stromberg. *Real and Abstract Analysis*. Springer Verlag, 1969.
12. C. Jordan. Sur la série de fourier. *C. R. Acad. Sci. Paris Sér. I Math.*, 92(5):228–230, 1881.
13. R. Kimmel and A. M. Bruckstein. Global shape from shading. *CVIU*, 62(3):360–369, 1995.
14. R. Kimmel, N. Kiryati, and A. M. Bruckstein. Distance maps and weighted distance transforms. *Journal of Mathematical Imaging and Vision*, 6:223–233, May 1996. Special Issue on Topology and Geometry in Computer Vision.
15. A. S. Kronrod. On functions of two variables. *Uspehi Mathematical Sciences*, 5(35), 1950. In Russian.
16. R. Kruse and A. Ryba. *Data structures and program design in C++*. Prentice Hall, New York, 1999.
17. H. Lebesgue. *Leçons sur l'Intégration et la Recherche des Fonctions Primitives*. Gauthier Villars, 1928.
18. I. P. Natanson. *Theory of Functions of a Real Variable*. Frederick Ungar Publishing, New York, 1964.
19. S. Osher and L.I. Rudin. Feature-oriented image enhancement using shock filters. *NumAnal*, 27(4):919–940, 1990.
20. P. Perona and J. Malik. Scale-space and edge detection using anisotropic diffusion. *PAMI*, 12(7):629–639, 1990.

21. L.I. Rudin and S. Osher. Total variation based image restoration with free local constraints. In *Proc. ICIP*, pages 31–35, 1994.
22. L.I. Rudin, S. Osher, and E. Fatemi. Nonlinear total variation based noise removal algorithms. *Physica D*, 60:259–268, 1992.
23. J. A. Sethian. *Level Set Methods and Fast Marching Methods*. Cambridge University Press, Cambridge, UK, 2 edition, 1999.
24. J. Weickert. *Anisotropic Diffusion in Image Processing*. Teubner, 1998.
25. J. Weickert. Efficient image segmentation using partial differential equations and morphology. *Pattern Recognition*, 34(9):1813–1824, 2001.
26. J. Weickert, B.M. ter Haar Romeny, and M.A. Viergever. Efficient and reliable schemes for nonlinear diffusion filtering. *IP*, 7(3):398–410, March 1998.